

OVERVIEW

Review on model development techniques for dam break flood wave propagation

P. D. P. O. Peramuna^{1,2}  | N. G. P. B. Neluwala²  | K. K. Wijesundara²  |
S. DeSilva¹  | S. Venkatesan¹  | P. B. R. Dissanayake² 

¹School of Engineering, Royal Melbourne Institute of Technology University, Melbourne, Australia

²Faculty of Engineering, University of Peradeniya, Peradeniya, Sri Lanka

Correspondence

P. D. P. O. Peramuna, School of Engineering, Royal Melbourne Institute of Technology University, Melbourne, Australia.

Email: s3894925@student.rmit.edu.au

Funding information

School of Engineering, RMIT University, Australia; Faculty of Engineering, University of Peradeniya, Sri Lanka

Edited by: Thomas Hartmann, Associate Editor, Nigel Wright, Senior Editor and Wendy Jepson, Editor-in-Chief

Abstract

Catastrophic failure of dam structures has often led to severe consequences. The colossal wave receding at a higher velocity from the sudden failure of the dams may obliterate the downstream areas causing loss of lives and property damage. Thus, proper mitigation measures and contingency plans must be formulated beforehand to minimize the impact of such disasters. Consequently, there has been a strong tendency to study dam breach flood modeling using different approaches for both hypothetical dam breach scenarios and real incidents. The technology used for dam breach studies is advancing and a comprehensive review of the existing methodologies would help the modelers in their model development. This paper reviews the state-of-the-art methodologies utilized in studies to propagate the dam break flood wave. Furthermore this guides the selection of methods best suited considering the project-specific requirements and the complexity of project to simulate the risk to the vulnerable areas generated from the dam break flood flow. Different terrain datasets, mesh generation techniques and calibration techniques have been adapted and adhered to improve computational accuracy, stability and efficiency in modeling dam break floods. The use of high-resolution global and site-specific datasets, subgrid models, the choice of roughness coefficients and high-resolution time steps have to be investigated thoroughly in these models. The paper reviews the existing methodologies with the strengths and limitations facilitating the future dam breach modelers to select the suitable approach in dam break flood wave modeling.

This article is categorized under:

Engineering Water > Sustainable Engineering of Water

Science of Water > Water Extremes

Water and Life > Conservation, Management, and Awareness

KEYWORDS

calibration, dam break, DEM, mesh, surface roughness, time step

1 | INTRODUCTION

Dams have been constructed across rivers for water storage, flood control, hydroelectricity generation and recreational purposes. Nevertheless, records of dam failures have been reported in many parts of the world, such as the failure of St. Francis dam and Malpasset dam, causing colossal damage to the ecosystem, buildings, infrastructures, road network systems and have affected thousands of lives. Furthermore, numerous dams all over the globe have nearly reached the estimated design life drawing public attention to the safety of the dams in the recent past (Albu et al., 2020).

Floods due to dam breaks are the most catastrophic flash flood events recorded worldwide (Psomiadis et al., 2021) compared with other precipitation runoff floods and second only to Tsunamis with the severity of impact and possibility of warning and evacuation (Jonkman & Vrijling, 2008). In general, dam break floods are sudden and massive, in which an uncontrolled, immense volume of water impounded by the dam structure will be mobilized at high speed within a short duration. Usually, the magnitude of the flow greatly exceeds the expected runoff floods from rainfall and the response time is remarkably shorter than for other precipitation-generated floods. In addition, dam failures introduce a known volume of water at a point located in a stream network and are short-lived with a rapid variation of pressure and velocity in both time and space (Carrivick, 2010), which significantly differentiate its devastating potential from other floods. In Ozmen-Cagatay et al. (2022), dam breach floods are characterized hydraulically as unsteady, non-uniform, nonlinear, and rapidly varied flow phenomena similar to a Tsunami. As a consequence, the momentum of the developed dam breach flow would create a high impact force in the downstream areas.

The above discussions warrant a risk assessment of a dam break via modeling, an essential component of dam safety programs supporting emergency response and risk management. Flood arrival time, flood velocity, peak flow discharge and the water surface elevation in the floodplain along with the distribution of flood depth at downstream locations routed in the floodplain (Figure 1) will be determined from the output of the dam break wave propagation modeling studies which would facilitate developing hazard maps that highlights the area vulnerable or affected by the dam break flow. In general, both the prediction of dam break hydrograph and the dam break flood routing are vital to quantify the hazard and risk of dam failures, which guides the formulation of emergency action plans that specifies pre-planned actions to minimize the impact to population and infrastructure (Bhandari, 2017; Zhong et al., 2019). The prediction of dam break hydrograph has also been critically analyzed in literature which depends on various characteristics such as material, geometry and capacity of dams and thus will not be discussed in this paper.

Accurate representation of the exact phenomenon of dam breach flow is challenging due to the complex and chaotic nature of flooding which is associated with a higher uncertainty. However, having a better numerical solution using the latest technology is the ultimate target of a hydrodynamic model. Besides, uncertainties exist in models which might account for the variations between model predictions and observed or real-world data. Sources of uncertainties are principally included in the design of the model itself (Bellos, Tsakiris, et al., 2020), considered parameters and input data (Kim & Sanders, 2016). The underlying computational equations govern the model geometry in which Shallow Water Equations are used for 1D and 2D models, whereas Reynolds Averaged Navier Stokes equations (RANS) are

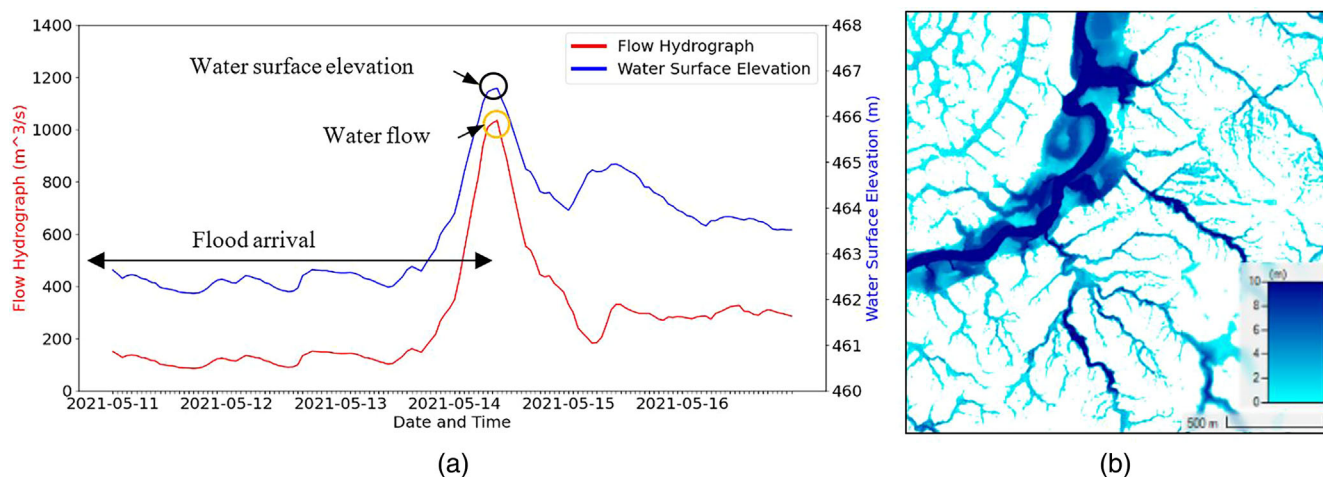


FIGURE 1 Flood arrival time, peak flow discharge and water surface elevation at a location for a specific flood event (a) and water depth distribution map in the downstream floodplain (b).

mainly used for 3D models. Furthermore, the literature discusses different numerical discretization methods and schemes that are employed in dam breach wave modeling associated with model geometries (Garcia-Navarro et al., 1999; Gottardi & Venutelli, 2004; Luo et al., 2019; Macchione & Viggiani, 2004, March; Quecedo et al., 2005; Robb & Vasquez, 2015; Shigematsu et al., 2004; Xanthopoulos & Koutitas, 2010; Yang et al., 2007). However, there needs to be more guidance in the selection of parameters in developing a model to facilitate the routing of the dam-break flood wave generated after the dam-break progression in the dam. Hence, this review paper is focused on the selection of parameters and input data for 1D and 2D model geometries, such as underlying terrain data, mesh size, boundary conditions, surface roughness and time step to reduce the uncertainty as exact representation is unrealistic in hydraulic models. The parameters related to 3D hydrodynamic simulations will not be discussed as those models are highly data intensive (Li et al., 2021) and computationally intensive (Zhang et al., 2018), thus, not frequently available for researchers all around the globe. In fact, dam breach flood modeling for a particular dam is very case specific. Thus, the parameters such as terrain, mesh size, boundary conditions, surface roughness and time step must be carefully analyzed in order to choose the most appropriate input data that could produce more reliable results. These factors have also been shown to be critical when analyzing the recalculations of the major dam disasters; to name a few are; Vajont dam disaster (Bosa & Petti, 2013), Gleno dam break (Pilotti et al., 2011), Saddle dam break of Xe-Pian Xe Nammoy reservoir (Latrubesse et al., 2020) and Cancano dam failure (Pilotti et al., 2020).

In model development of dam breach wave modeling, terrain data were first input to the model as it defines the characteristics of the land in which the flood flows and thus, terrain resolution is a critical parameter that influences the accuracy of dam breach studies (Ongdas et al., 2020; Wang et al., 2016). Although high-resolution datasets are encouraged in the literature for dam breach studies (Bornschein, 2018; Psomiadis et al., 2021), this paper comprehensively reviews the terrain datasets used for dam breach models, which are available worldwide and site-specific. Subsequently, meshing will define the terrain characteristics in a particular grid space and the mesh generation plays a vital role as the models are more sensitive to mesh resolution in complex terrains. Hence, this review critically analyses the techniques by guiding the selection of the optimum meshing type that would help the modelers to optimize the simulation time (Lakhlifi et al., 2018; Ongdas et al., 2020; Zhang et al., 2018). After that, boundary conditions discussed in the literature that were used in defining the inflow and outflow characteristics are evaluated, especially concerning hypothetical and real incidents. The surface roughness defines the resistance to the flow in the terrain and is helpful in calibrating the hydrodynamic models. Moreover, the time step defines the time intervals for the numerical discretization of underlying equations of the hydrodynamic models, which affects model stability and efficiency. These two essential parameters are critically evaluated in relevance to the existing literature. In addition, the use of calibration and validation of the model to further improve the accuracy by reducing the uncertainty of model prediction for a non-idealized environment (Lavoie & Mahdi, 2017; Macchione et al., 2016; Nkwunonwo et al., 2020; Ongdas et al., 2020) are investigated with the challenges and prospects for the future of dam breach flood modeling.

Thus, extending the aforementioned works, the paper systematically analyses the research in the last decade as presented in the peer-reviewed scientific literature, which particularly addresses new concepts in the context of state-of-the-art dam breach flood routing techniques and required data. Furthermore, this paper evaluates their applications, limitations, and validity which would facilitate the interested parties to choose the best approach to accomplish their requirement balancing the demands against model complexity, site characteristics, budgetary constraints and data requirements. The current review is organized in the following sections. The terrain datasets that can be used for dam breach modeling are first evaluated. The meshing techniques and subgrid models are then presented along with local mesh refinement. The boundary conditions that are used in dam breach studies are then evaluated. Techniques used in denoting surface roughness are analyzed before the evaluation of the time step in the next section. Next, the elimination of uncertainty through calibration is discussed. Finally, conclusions are drawn by summarizing key findings.

2 | TERRAIN DATA

Terrain surface on which the dam breach flood flows has to be accurate or closely represent the real domain in order to produce reliable model predictions closer to the exact situation. In 1D models, cross-sections generated from different topographic maps are used, whereas 2D models use a Digital Elevation Model (DEM) which is a 3D digital representation of the terrain surface in a gridded format where each pixel value corresponds to a height above a datum (Figure 2). DEM is an umbrella term to describe two types; DTM and DSM, where Digital Terrain Model (DTM) represents the bare earth and Digital Surface Model (DSM) represents the top elevation of buildings, canopy (vegetation) and water

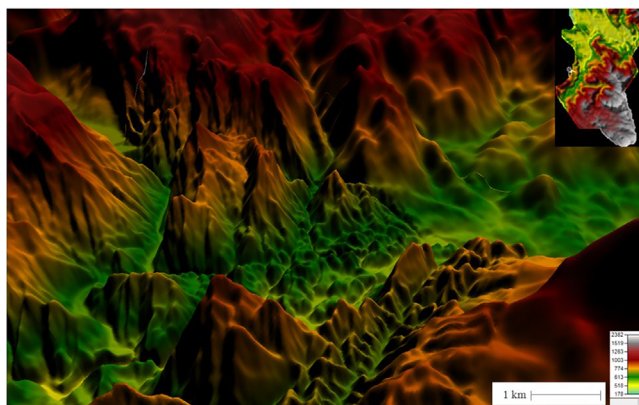


FIGURE 2 DEM of resolution of 1 m representing the topography of a part of Mahaweli basin in Sri Lanka obtained from the Survey Department of Sri Lanka.

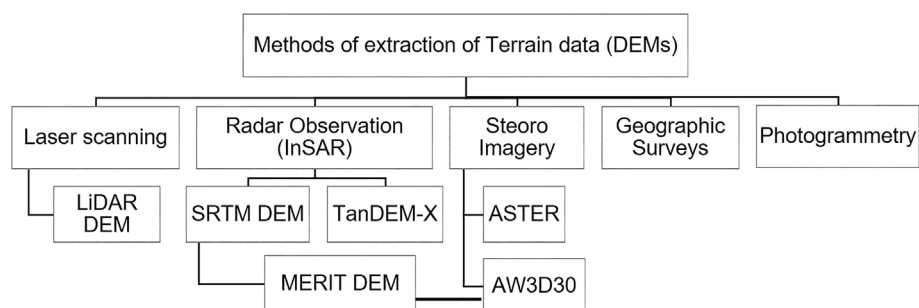


FIGURE 3 Methods of extraction of terrain data.

surface. The terrain datasets that are used in dam breach studies are available in formats of DTMs or DSMs. Psomiadis et al. (2021) have compared a high-resolution DSM obtained from aerial images and DEM obtained from orthophoto images in a dam breach study. It has shown considerable deviations between the results as high resolution DSM has captured surface relief and the existing natural obstacles accurately, which affects the flood routing significantly. However, anthropogenic elements such as houses, embankments, buildings and the natural vegetation represented in the DSM may be destroyed and drift away depending on the capability for flood resistance (Latrubesse et al., 2020). Furthermore, due to the presence of artificial structures on the terrain, there can be irrational peaks and depressions on the surface which creates nonphysical pools of water. Besides, with the change of 2D geometries of DSM during wave propagation, the use of DTM might be more reliable. Moreover, DTM utilizes lower computational power to store and process the data compared to DSM (Psomiadis et al., 2021). Therefore, further research must be conducted on the suitability of DSM and DTM for dam break flood modeling specially for an urban area because dam break floods are characterized by higher hydraulic energy than normal run-off floods due to precipitation.

Digitized maps from the existing maps drawn based on geographic surveys have been used in most of the recalculation of major dam disasters as those were the only available terrain datasets for the study area at the time (Alcrudo & Mulet, 2007; Belikov, & Vasil'eva, E. S., 2020; Hervouet & Petitjean, 1999; Valiani et al., 2002). Currently, the existing geographic maps are combined with other high resolution terrain datasets (Belikov, & Vasil'eva, E. S., 2020) developed from remote sensing methods (Figure 3) or the latter is used entirely. Remote sensing methods are less time consuming from data collection to data release, can generally be current up-to-date and as well as less expensive in some situations. In fact, the high-resolution datasets obtained from remote sensing have partly fueled the use of fine-scale modeling and 2D modeling (Macchione et al., 2016).

Under laser scanning, an Airborne Light detection and ranging (LiDAR) survey can be used to develop DSM with the elevation of above ground-features that return a signal to the laser pulse and subsequently has to be filtered to produce DTMs (Schubert et al., 2008). This has been first used for flood modeling studies as it provides high point density and remarkable height precision well suited for capturing floodplains (Mandlbürger et al., 2009). Due to the high resolution of LiDAR, it has produced more accurate results and is now extensively used if available for the study areas

(Gallegos et al., 2009; Urzic  et al., 2021). In fact, LiDAR technology is not dependent on shadow conditions during the data collection process and has higher precision and accuracy owing to its reduced vulnerability to scatter (Albu et al., 2020). However, aerial LiDAR has difficulty detecting floodwater passages under urban structures such as sky-train tracks or crosscutting alleyways and therefore suggested using with Structure from Motion (SfM) approach (Meesuk et al., 2015). Thus, LiDAR requires specific technology and skill for collecting and preprocessing, thus can be expensive to acquire and limited mainly to a handful of countries (Ali, 2016; Courty et al., 2019).

Furthermore, topography data created using Structure-from-Motion (SfM) photogrammetry using Unmanned Aerial Vehicles (UAVs) is an emerging technology with a relatively lower cost than LiDAR. Here, aerial images are captured with an overlap and cameras that capture visible light (red, green, and blue; RGB) is used despite having limited spectral resolution. Such dataset has been used in the dam breach study of Psomiadis et al. (2021) and in dam removal studies (Evans et al., 2022). Furthermore, this might be a useful dataset in the creation of a 3D virtual environment for communicating the dam breaks in the future, as discussed in Spero et al. (2022). However, this dataset is costly compared to global datasets and requires special technology and skills to acquire the data.

On the other hand, Spaceborne Interferometric Synthetic Aperture Radar (InSAR), is the most common technique to create global DEMs and the technology behind the widely used open-access global DEM, Shuttle Radar Topographic Mission (SRTM) (Farr et al., 2007; Rabus et al., 2003). SRTM has terrains of 1/3 arc second (10 m) which is available for the USA and 1 arc second (30 m) and 3 arc seconds (90 m) which are available for most of the globe. Bhandari (2017) has used 1/3 arc second SRTM (10 m resolution) for the dam failure event of Big Bay dam located in Lamar county, Mississippi and has shown satisfactory results. The latest SRTM DEM of 1 arc second (30 m) can be downloaded for free of charge from the United States Geological Survey (USGS) Earth Explorer website (was made available after 2015), making it the most accurate and frequently used topographic data (Kim & Sanders, 2016; Patel et al., 2017). Kim and Sanders (2016) stated that the selection of SRTM must be done considering the topography and spatial scale of both the river channel and the floodplain. Because in that dam breach study where the flood width of the study was on the order of 1 km, raw SRTM data has not been helpful and has shown a 20% under prediction of flood extent. Therefore, SRTM is more suggested for larger areas and high magnitude floods. Moreover, canopies of dense forests are detected by radar in SRTM. Hence, it requires supplementary processing based on in-field data, especially in areas with different vegetation density values which earlier possessed low vertical accuracy (Albu et al., 2020;  lvarez et al., 2017). Therefore, new topographic datasets based on SRTM data are developed by eliminating the drawbacks. For example, O'Loughlin et al. (2016) have developed a global Bare-Earth DEM by correcting the vegetation bias in the original SRTM which has a resolution of 90 m.

TanDEM-X DEM (TerraSAR-X add-on for Digital Elevation Measurement) is the other dataset that used InSAR (SAR X Band) and produced DEM with the resolution of 12 m (0.4 arc second—commercial product), 30 and 90 m (Grohmann, 2018; Krieger et al., 2007). In TanDEM-X DEMs, data have been acquired using two SAR satellite images (bi-static acquisition mode) simultaneously with short along-track baselines. TanDEM-X DEM has been used for ice dam breach modeling studies (Scapozza et al., 2019) and for flood modeling studies (McClean et al., 2020), but not yet in a dam breach modeling study, according to the author's knowledge.

DEM developed from Advanced Space-borne Thermal Emission and Reflection Radiometers (ASTER) and Advanced Land Observing Satellite (ALOS World 3D-30 m) (AW3D30) are global datasets that are developed using optical satellite images. However, due to the lower accuracy or higher terrain errors of ASTER DEM compared to SRTM DEM, it has not been used frequently for flood modeling studies (Courty et al., 2019; Farooq et al., 2019). ALOS World 3D-30 m (AW3D30) (Tadono et al., 2014) was released in May 2016 by the Japan Aerospace eXploration Agency (JAXA). This dataset is created using the images of the PRISM panchromatic stereo mapping sensor taken between 2006 and 2011. In fact, AW3D30 has been derived from the commercially available 5 m DEM (AW3D DEM), which can be either obtained as a DTM or a DSM. Courty et al. (2019) have compared the performance of ASTER, SRTM and AW3D30 in two catchments and AW3D30 has performed better than SRTM and ASTER in representing the terrain, especially in steep slopes. However, ALOS World 3D-30 m has not been extensively used in dam-break flood modeling studies. Nevertheless, a new version (i.e., version 3.2) was released in 2021 and this new version will be influential in developing better dam breach models in the future.

Multi-Error-Removed Improved-Terrain (MERIT) DEM (Yamazaki et al., 2017; Yamazaki et al., 2019) is another global dataset developed based on SRTM DEM, AW3D30 DEM. It has been corrected and adjusted according to hydrologic and hydraulic features with removal of vegetation canopy having the highest vertical accuracy out of the global datasets (Latrubesse et al., 2020; Yudianto et al., 2021). Latrubesse et al. (2020) have utilized MERIT DEM to identify the shorelines of the reservoir for the dam breach model, while Yudianto et al. (2021) have utilized it to create dam breach hazard maps in data sparse regions.

The use of globally available topographic data becomes a viable alternative with necessary corrections and accuracy assessments in the absence of other topographic data, such as in the dam breach studies of Álvarez et al. (2017) and Yudianto et al. (2021). Overall, most of the global datasets (Table 1) have World Geodetic System- 1984(WGS84) as the horizontal coordinate system. The common vertical reference system has been the Earth Gravitational Model 1996 (EGM96 GEOID) based on the ellipsoid specified by WGS84 except for TanDEM-X DEM. The vertical resolution is expressed in many formats such as Mean Absolute Error (MAE), Root Mean Square Error (RMSE) and linear error at 90% confidence level (LE90) which defines the uncertainty in the height of a pixel for a reference height caused by random and uncorrected systematic errors. In conclusion, the use of the highest resolution topographic dataset is more advisable if it is available for the dam breach study area considering the budgetary requirement and intended use. However, the contribution from global datasets in providing terrain data with good accuracy cannot be neglected.

3 | MESH DEVELOPMENT

After the introduction of terrain, the boundary of the presumed flood domain has to be added to the model. This flood domain will be represented as a series of cross-sections along a channel profile in a 1D model or as a mesh in the domain of a 2D model (Figure 4). At first, the delineation of the domain for a hypothetical dam breach can be challenging as the flood extents are unknown. Hence, it is suggested to define a domain based on engineering judgment and to conduct a preliminary flood simulation with a coarser extent. Afterward, mesh refinement can be iterated to the wetted portions of the domain to achieve convergence (Begnudelli & Sanders, 2007; Gallegos et al., 2009).

In Pilotti et al. (2014), 1D models have been used to analyze dam break wave propagation and the effect of cross sections with different cross-sectional spacing has been investigated for a 16 km long river stretch. Models with four

TABLE 1 Summary of global datasets used for dam breach modeling studies in which DSM is denoted with ‡ and the datasets which have both DSM and DTM is denoted in • and commercial software is denoted with *.

Dataset	DTM/ DSM	Coverage	Link for the datasets	Horizontal resolution (m)	Vertical resolution (m) and reference system
SRTM DEM	‡	56° S–60° N	Earth explorer website (https://earthexplorer.usgs.gov/)	30,90	6 (MAE) WGS84 (EGM96 GEOID)
ALOS World 3D-30 m (AW3D30)	‡	82° S–82° N	ALOS Research and Application Project website (https://www.eorc.jaxa.jp/ALOS/en/aw3d30/data/index.htm)	30	4.4 (RMSE) WGS84 (EGM96 GEOID)
ALOS World 3D-5 m (AW3D)	•	82° S–82° N	AW3D Website (https://www.aw3d.jp/en/)	5*	2.7 (RMSE) WGS84 (EGM96 GEOID)
TanDEM-X DEM	‡	Entire earth	TanDEM science service system (https://tandemx-science.dlr.de)	12*, 30, 90	10 (LE90) WGS84-G1150
MERIT DEM	DTM	60° S–90° N	MERIT DEM Website (http://hydro.iis.u-tokyo.ac.jp/~yamada/MERIT_DEM/)	90	5 (LE90) WGS84 (EGM96 GEOID)

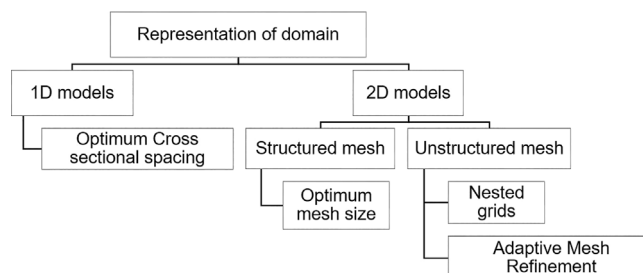


FIGURE 4 Categories of meshing.

different resolutions with mean spacing 130, 24.4, 12.2, and 3.3 m (the number of cross-sections are 125, 667, 1332 and 4987 respectively) derived from 30 m resolution DEM have been compared. The results have shown that flood hydrographs from all the models converged to the results of mean spacing of 12.2 m. This result implies that lowering the mesh size (3.3 m mean spacing in this case) beyond a specific mesh size (12.2 m mean spacing in this case) has no specific contribution to improving model accuracy. In addition, it shows that coarse resolution smoothens the bed irregularities, causing a faster flood arrival time for a dam breach. This implies the effect of fine mesh on the final results in 1D models and the importance of selecting an optimum mesh size.

In a 2D model, a mesh will be created by discretizing the space to small geometrically simple elements. The selection of optimum mesh resolution can be seen among structured grids, whereas site-specific mesh refinement can be seen in unstructured grids (Kim et al., 2014). The ability of unstructured mesh to provide local mesh refinement where needed leads to improved accuracy for a given computational cost compared to structured mesh (Lakhlifi et al., 2018). The structured meshes will be beneficial due to the smaller model setup time and in the absence of additional data for large-scale simulations (Shustikova et al., 2019).

In the 2D dam breach study of Albu et al. (2020), different cell sizes were analyzed, starting from square grids of 30 m for an area of 943 km² and reducing with 5 m decrements up to a mesh cell size of 1 × 1 m². Here, 20 × 20 m² mesh cell size was found to be optimum in which the accuracy does not significantly change but with a reasonable computational time. Hence, the cell size of 19 m which was slightly below the threshold, was selected as the model mesh size. Similarly, in the dam breach study of Pilotti et al. (2020), where the mesh sizes of 60, 30, 20, and 15 m were analyzed for a 15 km distance of river stretch, it shows that 20 m cell size has the most reasonable accuracy and the computational time. In fact, the wave arrival time and the peak discharge were almost insensitive to the average mesh sizes less than 30 m which includes mesh sizes of 20 and 15 m. Furthermore, both mesh sizes of 20 and 15 m produced similar results and were in good agreement with experimental results. However, modeling with fine-structured mesh (15 m) has taken a longer computational time of about 2.5 times greater than that of the 20 m.

In conclusion, using an optimum resolution in cross-sections and in the mesh is significant, and simulations must be planned considering the sought numerical precision, stability, run-time execution costs, resolution of available topography data and budgetary constraints.

3.1 | Approaches in the refinement of the mesh

When significant structures such as river banks, roads and buildings are present, the obstructions and depressions affect the flow pattern or propagation. Hence, in order to capture their effect, the mesh has been refined by aligning and inserting cells accordingly in an unstructured grid (Gallegos et al., 2009; Wang et al., 2020). In other words, small elements may be used in areas where more details are desired, and larger elements are used where fewer details are needed, optimizing information for a given amount of computational time.

Some software such as SOBEK and HEC RAS have nested grids in which a fine mesh known as child mesh can be within another mesh (parent mesh). In this method, more cells with small sizes are placed along critical terrain while a higher mesh resolution exists in homogeneous areas, making it possible to vary the grid size. However, this would create problems related to stability as a small-time step has to be used for the entire domain satisfying the Courant condition (section 6.0). In fact, mesh refinement has been significant in urban flood modeling studies (Schubert et al., 2008) and in dam breach studies. The researchers have utilized smaller mesh near the dam area and flood path while placing larger mesh sizes where significant local surface variances are not observed mainly to reduce the computational time and achieve sufficient accuracy (Álvarez et al., 2017).

Another approach that can be used is Adaptive Mesh Refinement (AMR, locally nested static mesh method or temporal refinement (Baeza & Mulet, 2006), which provides greater accuracy and does not demand excessive computational resources. AMR typically uses element subdivision (Figure 5), where a set of coarse mesh patches covers the whole domain. The sub-division of groups of coarse cells is repeated, such that grids at different resolution levels coexist. Each mesh patch can be viewed in isolation and can be integrated independently and confined for a small part of the domain, so the time step used at the coarse grid will not be restricted (Baeza & Mulet, 2006). With adaptive meshes, a high resolution is automatically obtained in regions where the gradients of the water depth are steep, such as the moving fronts with higher accuracy (Lakhlifi et al., 2018).

Garcia and Popiolek (2014) and Lakhlifi et al. (2018) have used an adaptive triangular mesh to model the dam break flood flow path and have achieved a high precision solution at a low computational cost. Lakhlifi et al. (2018) have

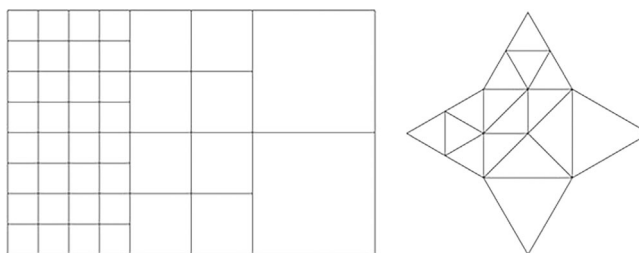


FIGURE 5 Sub-division of coarser cells in adaptive mesh refinement.

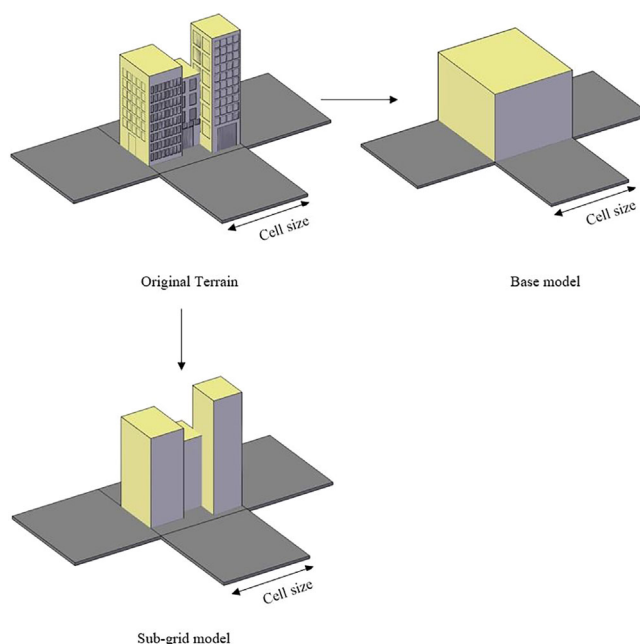


FIGURE 6 Representation of terrain using the base model and subgrid model.

shown that adaptive mesh has saved more than 70% of CPU time compared to a refined model in the domain, which has used a total CPU time of 1534 s. Thus, mesh refinement, especially in the area near the vicinity of the dam, can be used to improve the model performance in dam breach studies.

The necessity to analyze the interaction of the flow with other man-made elements, such as bridges or flood barriers as the piers, is highlighted as it might provoke backwater effects. This might create significant variations in water elevation on the cross-section together with variability of flow properties within the cross section (Costabile et al., 2015). Macchione et al. (2016) have studied the effects of bridges and found that the maximum difference in the computation of water surface elevations between the models with and without bridges is less than 1 m (i.e., 0.81 m) and it is only a local effect which has occurred just upstream of the Roadway Bridge. Thus the study concluded that bridges have a limited influence on that particular dam breach flood flow, likely due to the limited narrowing induced by piers located in the riverbed. Furthermore, the effect of bridges and infrastructure are not considered in most dam breach studies may be due to the limited effect it has on the dam breach flood flow and as it is impractical to model every bridge and culvert in a larger domain given the unavailability of data on bridges (Ahmadian et al., 2018). However, the inclusion of the effect of bridges has to be considered by carefully evaluating the characteristics of the study area and the magnitude of the dam break event.

3.2 | Sub-grid bathymetry

Another approach to further increase the accuracy without further increasing the computational time is to use a sub-grid model in which coarser grids will automatically obtain fine scale details within a 2D cell in the underlying terrain and the simulation can be run for coarser mesh sizes (Figure 6) (Dasallas et al., 2019; Ongdas et al., 2020;

Pilotti et al., 2020). During a preprocessing step, hydraulic radius, volume and cross-sectional data are collected for each mesh cell using the finer resolution data and stored in property tables. Software such as HEC-RAS, TuFLOW, possess sub-grid bathymetry features and this technique can be used to improve computational efficiency. Shustikova et al. (2019) analyzed the effect of a $25 \times 25 \text{ m}^2$ grid with information of a $1 \times 1 \text{ m}^2$ terrain resolution. For the comparison model, a $25 \times 25 \text{ m}^2$ grid with information of a $25 \times 25 \text{ m}^2$ terrain resolution model was developed. In here, the terrain resolution was manually altered to match the mesh size. Similarly, models of 50 and 100 m grids were developed for both cases. The models with subgrid bathymetry have shown better predictions of inundation boundary, whereas the other models have produced plausible results in flood depth. However, the computational time is higher for the subgrid models in which a subgrid model of 100 m is takes four times of computational time than that of the model with 100 m mesh size with the 100 m terrain resolution.

In summary, mesh size plays a significant role in achieving accurate results for a reasonable computational time and therefore, special attention has to be paid in the selection of an optimum size.

4 | BOUNDARY CONDITIONS

According to Chow et al. (1998), flood routing is defined as the procedure to determine the time and magnitude of flood hydrographs at a point on a watercourse from known hydrographs at one or more points upstream. Hence, boundary conditions are utilized to define the inflow and outflow of the model for all model geometries. There are three main types of boundary conditions as shown in Figure 7. These can be assigned based on the historical data for recalculation of disasters or probability of natural disasters leading to modeling of hypothetical dam breaks.

Researchers have mainly used flow hydrographs based on experimental studies, real dam breach measurements or other dam break models and equations to denote the dam breach flood wave calculated based on reservoir water levels, as the upstream boundary conditions when developing models. Pilotti et al. (2014) and Pilotti et al. (2020) have compared the capabilities of different numerical models and have modeled the upstream boundary conditions of 1D and 2D simulation of Cancano dam failure by using a measured discharge hydrograph from an experimental study of the hypothetical Cancano dam breach conducted by De Marchi, (1945). De Marchi, (1945) created a physical model of 1:500 scale built in Froude similitude for the upper part of the valley and has provided discharge hydrographs that serve as validation test cases for numerical models. Moreover, Palu and Julien (2020) have used the dam breach flow hydrograph from the real dam break of Fundão Dam recorded by the National Water Agency in Brazil as the upstream boundary condition. This study has focused on testing and developing the 1D algorithms in a dam breach study.

For hypothetical dam breach failures or in the absence of real dam breach data or experimental data, upstream dam breach hydrographs must be generated. Mainly there are four methods to obtain the breach parameters and to estimate the dam breach flow which will highly influence the hydraulic model predictions. The analogy method in which comparative analysis is carried out with a similar dam that has been breached (Říha et al., 2020) and guidelines from different authorities that provide conservative upper bounds of breach parameters which are suitable in the framework of a deterministic risk analysis (Salt, 2019) are the first two methods. The other methods are the regression based methods

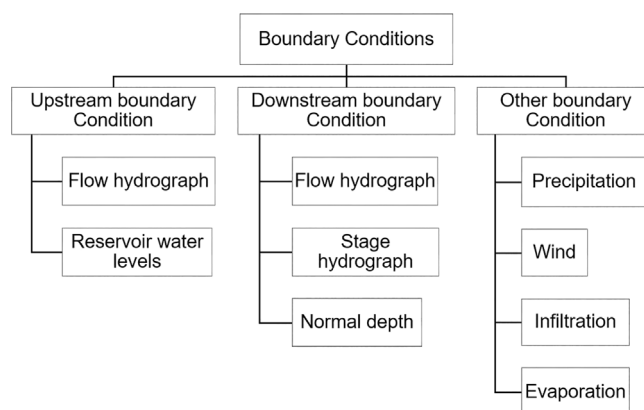


FIGURE 7 Categories of boundary conditions.

which are prediction formulae based on statistical regressions obtained from a database of reported dam breach failures (Ahmadisharaf et al., 2016; Tedla et al., 2021) and physically-based simulation models calculating the erosion process to define the breach configuration and the breach flow estimations (Zhong et al., 2016). Bricker et al. (2017) have used BREACH, a physically based dam breach model based on the geometry and geotechnical properties of the dam to generate the upstream hydrograph at the landslide location in the 1D model. In fact, Říha et al. (2020) have performed a Monte Carlo sampling procedure to define the optimum dam breach parameters, such as geometrical and geotechnical properties of dams and reservoir levels, which was then used in models to derive the hydrographs with the highest peak outflow. Thus derived outflows have been compared with other real dam breach incidents and empirical equations for further verification. As the upstream boundary conditions, the dam breach flood hydrograph for the worst-case scenario has been used near the dam and hydrological flood hydrograph at the local streams has been used for the 2D simulation.

In all the methods uncertainties affecting the predictions remain high and they are mainly based on dam geometry, construction materials and reservoir levels rather than the probabilistic occurrence of the natural hazards (Froehlich, 2008; Říha et al., 2020). Hence it is necessary to investigate the dam break configurations for different probabilities of natural disasters such as rainfall, earthquakes and landslides to reservoirs. However, in this paper the derivation of dam breach parameters or breach flow will not be discussed for the sake of brevity.

To define the outflow of water from the model (downstream boundary condition), normal depth can be used in addition to flow and stage hydrographs which are observed at gauging stations. In fact, normal depth is widely used for hypothetical dam breach failures as the exact flood conditions downstream are unknown and observed data are unavailable for real dam breaks while assuming the flow to be a normal flow (Bellos, Tsakiris, et al., 2020; Grover et al., 2013; Haltas, Elçi, & Tayfur, 2016; Palu & Julien, 2020). Normal depth is the depth of flow in a channel when the slope of the water surface and channel bottom is the same and the water depth remains constant. The friction slope has to be determined to input into normal depth calculation, and it is mostly taken as the average channel bottom slope from the topography (Haltas, Elçi, & Tayfur, 2016; Pilotti et al., 2014). Bellos, Tsakiris, et al. (2020) have done a model simulation for a hypothetical dam failure, assuming the friction slope as the average bottom slope of the stream, which is 0.02.

Alcrudo and Mulet (2007) and Macchione et al. (2016) have stated that the implementation of boundary conditions in a computational model plays an important role in the outcome of the simulation. This is due to the fact that if a downstream boundary condition is placed closer to the region of interest, boundary treatment is more noticeable (Alcrudo & Mulet, 2007). In other terms, the cells defining the boundary cells in a study area have to be located far from the point of interest, which might be the last observation of the watermark or a gauging station in order to eliminate the influence of the boundary condition on the results. Bricker et al. (2017) have used the normal depth far enough to be inconsequential with a slope of 0.007 in the 1D model.

The other boundary conditions are wind, evaporation, infiltration and precipitation and in new modeling software, the 2D variation of these parameters are calculated for the whole study area. In most dam breach studies, the effect of wind has not been taken into account, which might be due to the negligible effect of wind on the turbulent nature of dam breach flood flow. Moreover, the effect of evaporation and infiltration is assumed to be small and neglected, which is justified in cases where dams are overtopped by extreme rainfall events (Albu et al., 2020; Kim & Sanders, 2016; Patel et al., 2017; Tedla et al., 2021).

Dam breach studies have been conducted on the basis of wet day failures (Tedla et al., 2021) or sunny day failures where no rainfall is concerned (Álvarez et al., 2017; Salt, 2019). In Tedla et al. (2021), the precipitation data has been used for the generation of peak inflow hydrographs using HEC-HMS models and it has been used to simulate inflows to the dam. In some models, initial conditions have been input representing the water surface levels within the modeling area, taken at the beginning of the calculation (Kidyaeva et al., 2017). However, the choice of using an initial condition lies with the modeler.

5 | SURFACE ROUGHNESS

Surface roughness determines the frictional force exerted on the flood wave during propagation which is included in the shallow water equations (Cannata & Marzocchi, 2012). It is denoted by Manning's values based on the land cover, land use and vegetation density (Chow, 1959) and is considered a fundamental source of uncertainty (Yochum et al., 2008). Moreover, roughness coefficients are sensitive both to model geometry (1D and 2D models) and mesh

discretization (Pappenberger et al., 2005). Bornschein (2018) has shown that arrival time has been significantly affected by the roughness coefficient for a flood path of 25 km. Here, the flood wave is delayed by 26 min if a very rough surface is used for the flood path and the arrival time is 16 min shorter for a very smooth surface flood path. Furthermore, the difference between the flood arrival times in both surfaces tends to be very small during the first 4 km of the flood path. Hence the study concluded that the longer the propagation path the higher the uncertainty in flood wave arrival time due to uncertainties in Manning's n determination.

Earlier, a spatially uniform value of roughness coefficient has been used for the entire model domain upon calibration (Begnudelli & Sanders, 2007; Hervouet & Petitjean, 1999; Vacondio et al., 2016; Valiani et al., 2002). Begnudelli and Sanders (2007) have used a uniform value in the range of 0.02–0.03 $\text{m}^{-1/3}$ s which agrees with the study area, Southern California, which has sparse vegetation regions. Here, it is shown that upon calibration, the flooded area can be predicted within 4% and travel times can be predicted within 10% by adjusting a uniformly distributed Manning coefficient within reasonable limits. The study also suggests that more accuracy can be attained using spatially varying coefficients.

On the other hand, spatially distributed Manning's coefficient was assigned to each cell in accordance with a simple land cover classification (Figure 8) which is most suited for urban dam breach flood modeling (Gallegos et al., 2009; Marangoz & Anilan, 2022; Psomiadis et al., 2021; Sattar et al., 2019). Gallegos et al. (2009) have assigned Manning n values of 0.014, 0.016, 0.013, 0.30, and 0.050 $\text{m}^{-1/3}$ s to roads, channels, reservoirs, developed parcels with buildings, and vegetated open space, respectively based on manual land cover classifications. The higher Manning value for developed parcels with buildings has been selected based on expected flow obstruction as recommended by the United States Army Corps of Engineers (1981). When the model with spatially distributed Manning's coefficient was compared with the model of uniform Manning's coefficient (0.2 $\text{m}^{-1/3}$ s) for the domain, the former showed better predictions of peak flow and flood travel time, showing the necessity of distributed resistance parameters. Similarly, Bosa and Petti (2013) have used spatially varied coefficients and higher roughness especially in urban area to represent the flow resistance of the buildings.

Although the use of very detailed variations of the roughness values along each cross-section is allowed in 1D simulations, this is not recommended. The reason is that this can create problems in unsteady models, as abrupt changes of the roughness values can cause the model to become unstable. Hence in Grover et al. (2013), uniform Manning's n values were assigned for the overbanks ($n = 0.08 \text{ m}^{-1/3}$ s) and the main channel ($n = 0.035 \text{ m}^{-1/3}$ s). In the study of



FIGURE 8 Spatially distributed roughness coefficients based on land use land cover maps for a basin.

Vacondio et al. (2016), where urban and rural areas exist in the terrain, flow characteristics have not shown considerable sensitivity to the roughness coefficient in rural areas. In contrast, flow characteristics have been greatly influenced by the roughness coefficient for urban areas.

Shustikova et al. (2020), Albu et al. (2020) and Tedla et al. (2021), have used uniform roughness coefficients for channel bed and floodplain based on Chow's recommendation (Chow, 1959) to reduce the number of uncertain variables. However, as stated by Shustikova et al. (2020), the roughness coefficient has to be carefully selected as lower values near the dam might make the numerical models unstable. In contrast, Latrubesse et al. (2020) have shown that the influence of Manning's coefficient on water flow is negligible because of the high kinetic energy of the floodwaters, which makes frictional losses negligible in a dam breach flood flow. Although this is true near the dam in which the flood flow is governed by the reservoir pressure level or the depth of impounded water in the initial hydraulic flow regimes, later in the floodplain, the dam breach flow is governed by friction which is also influenced due to the increase of wetted perimeter (Carrivick et al., 2011; Sarchani & Koutroulis, 2022).

Generally, the calibration of the models is performed by varying floodplain roughness coefficients in order to reproduce the actual phenomenon (Pilotti et al., 2020; Shustikova et al., 2019). In Kim and Sanders (2016), the calibration of the roughness coefficient reduces the flood height RMSE to 0.33 m, which is close to the estimated uncertainty in flood height measurements (0.2 m) and RMSE of the best available topographic data (0.2 m). Furthermore, the roughness coefficient has been used to compensate for geometrical uncertainty to a certain degree which results from complex terrain features in a flood plain or river geometry that affects flood propagation (Cao et al., 2014) or to account for a high level of turbulence of the outflow from the dam breach which facilitate model's stability (Asnaashari et al., 2014). On that account, in some studies, the effect of such varying complex terrain features, meanders and secondary flows have been practically incorporated by utilizing an increment of roughness coefficients in the terrain (Bornschein, 2018; Cao et al., 2014).

In contrast, the roughness of the surface or the floodplain will be changed as rough elements and obstacles might wash away, making the water flow path smoother during the flow of dam break flood (Latrubesse et al., 2020). However, no studies were found to utilize the change of roughness during the simulation of dam breach flood wave propagation which will be highly beneficial in urban dam breach flood modeling. On the other hand, dam break floods are highly energetic volumes of water with sediment flow and relatively coarse sediments may be transported as suspended loads (Alcrudo & Mulet, 2007; Carrivick et al., 2011; Swartenbroekx et al., 2013). In fact, some of the dam break models have not considered sediments or mobile beds (pure water or clear dam break flows) (Pilotti et al., 2014) due to the idealization of only the presence and co-existence of varying hydraulic flow regimes with neglecting the insignificant effect of debris flow due to strong dilution by huge volume of water (Pilotti et al., 2011), absence of field measurements for verification (Carrivick et al., 2011), and due to uncertainty of floodplain sediment characteristics and modeling. This latter fact is seen in the dam break studies with mobile beds, where the soil is assumed as uniform and of the same diameter (Cao et al., 2014) or mobile beds are presented as double layer averaged models (Li et al., 2013). However, these techniques and formulations for sediment exchange in flow and bed will not be discussed in the paper for brevity.

6 | TIME STEP

The time step of the model has a higher influence on the total computational time as it denotes the time taken by the fluid to pass a cell (Lavoie & Mahdi, 2017; Ozmen-Cagatay et al., 2022). Large time steps would cause numerical diffusion and model instability in addition to attenuation of peak, whereas very small time steps would yield more computational time and possible model instability (Gaagai et al., 2022; Haltas, Tayfur, & Elci, 2016; Tedla et al., 2021). Hence, the convergence of the time step would be beneficial to increase the model performance which is best if it is small enough to let the flood water cross only one grid cell during the time step period. Hervouet and Petitjean (1999) used a time step of 0.5 s with a run of 8000 steps for the Malpasset dam breach and compared it with a time step of 1 s which showed an increase of 25% in flood arrival time.

In fact, both fixed time steps and variable time steps limited by a Courant–Friedrichs–Lewy (CFL) constraint can be used in dam breach modeling (Soares-Frazão et al., 2012). Variable time steps primarily improve stability and reduce computational time and this feature is enabled in software such as TELEMAC-2D, HEC RAS for 2D models (Grover et al., 2013) as well as in 3D models (FLOW-3D). In here, the time step is automatically adjusted by respecting the Courant–Friedrichs–Lewy (CFL) stability criterion (Ozmen-Cagatay et al., 2022). Pilotti et al. (2020) used a variable time step for the 2D model to advance the simulation in time.

The time step is related to the mesh size and flood wave speed that can be derived from the Courant–Friedrichs–Lewy condition (Bellos & Sakkas, 1987; Courant et al., 1967):

$$C = \frac{V\Delta t}{\Delta x} \quad (1)$$

where, C = Courant number (dimensionless), Δt = time step, Δx = grid cell size and V = flood wave velocity.

A Courant number less than or equal to one is recommended for model stability (Asnaashari et al., 2014; Vacondio et al., 2016). The typical time steps for dam break simulations are recommended to be in the range between 1 and 60 s (Brunner, 2020). Albu et al. (2020) have conducted dam break simulations with different dam break sizes such that each dam break simulation is observed for 20 h. Hence, in order to computationally optimize the modeling process, first simulations with an arbitrary time step of 30 s have been conducted for dam breach sizes of 1%, 10%, and 100% and for the same mesh size of 19 m (discussed in Section 3). This was carried out in order to identify the average water velocity for different dam breach scenarios. Subsequently, an average water velocity was extracted for these dam breach sizes and multiplied by 1.5 (Brunner, 2020) to identify the flood wave speed. Next, Courant values have been obtained by incorporating thus calculated wave speeds with the mesh cell size of 19 m and arbitrary time step values of 10, 20, and 30 s. The time step which resulted in a Courant value lower than 1 was chosen for simulations such that 10 s has been used for 100% breach size, 20 s for breach sizes from 5% to 90% and 30 s for 1% breach size. Moreover, for the historical model simulation in the levee breach study of Shustikova et al. (2020), a computational time step of 5 s has been used for the 100 h event simulation. In this model, the mesh size is 25 m and simulated approximately for a 50 km² floodplain. The dam breach studies that focused on verifying different numerical schemes using both model and experimental flows in the near vicinity of dams have used smaller time steps of less than 1 s for simulation. Cannata and Marzocchi (2012) have run the simulations for 8 s with a time step is 0.01 s. Here, the computational domain is a square of 200 m and a cell size of 5 m. The research intention was to find the capability of a particular numerical scheme in modeling dam breaks. Bricker et al. (2017) have used a time step of 0.01 s to validate the Delft-FLOW model using the recorded data of the Malpasset dam breach in Hervouet and Petitjean (1999) for mesh sizes between 20 and 7.5 m. Therefore, in conclusion, most of the dam breach studies have used smaller time steps considering the high velocity of the dam break flood wave and smaller cell sizes used to propagate the flood in the domain. However, the time step has to be chosen based on the engineering judgments considering the mesh size, total simulation time, flood velocity and model characteristics such as dam break study area and model intentions.

7 | REDUCTION OF UNCERTAINTY THROUGH CALIBRATION AND VALIDATION

Calibration is the method of post-processing a model to improve the probability estimate (Tedla et al., 2021) and validation verifies that the developed models accurately represent the real world situation. In calibration, the model performance is checked using historical events or experimental data (Pilotti et al., 2020) and iterates the model until the desired accuracy is achieved by refining the model parameters within the acceptable parameter bounds. Comparison of model results with the recorded observations has to be done for several events during calibration. Thus, calibrated model is validated using the recorded observations for another set of flood events. The data types for calibration and validation can be identified as surveyed peak flood levels, maximum height gauges, water marks on buildings and debris lines, continuous water level gauges, velocity gauging, anecdotal evidence and flood extent aerial imagery, which can be derived from pictures, videos, satellite images and reports available on the Internet and through in situ interviews (Azeez et al., 2020; Bricker et al., 2017; Vacondio et al., 2016). Hence, collecting and cataloguing these data immediately after a dam breach event is preferred. According to Begnudelli and Sanders (2007) and Pilotti et al. (2011), calibration was done mainly concerning the arrival time in several dam break inundation studies that considered actual events. In some instances, data available after a dam breach, such as maximum water depths, watermarks, and extent of flooded areas, will be adequate for calibration.

Calibration is not feasible for a hypothetical dam-break flood model in which the solutions are required before an actual dam-break occurs. In addition, data might not be available in past dam breach events as catastrophic dam events may not be frequent, and available data might not be complete or entirely accurate (Aureli et al., 2021) or virtually absent when the measuring instruments and equipment are not prepared for extreme events (Farooq et al., 2019;

Jančíková & Unucka, 2015). Thus, to eliminate the parametric uncertainty, the results can be evaluated using experimental data from physical models (Haltas, Elçi, & Tayfur, 2016; Pilotti et al., 2020) or by calibration and validation of parameters for historical flood events in the same study area (Mhmood et al., 2022; Yudianto et al., 2021). In the latter, the model is first calibrated for a flood model and then used for the dam breach study.

For hypothetical dam breaks, as no such real events are recorded, data on previous flood events would be beneficial in model calibration. In Mhmood et al. (2022), the roughness coefficients of the model for the study area have been calibrated based on the flood in 1980 that happened in the same study area. Upon the calibration of Manning's values, the water stages have been compared with observations for nearly 2 months (May 1, 2008 to June 30, 2008) to validate the selected parameters. After that, the model was used to simulate hypothetical dam failure. Moreover, Shustikova et al. (2020) tested the sensitivity of model parameters using an upstream hydrograph observed for a historical levee breach simulation at a gauging station located 5.5 km upstream of the breach location before using it in the dam break simulation.

On the other hand, physical models can be constructed to calibrate the numerical models and as well as to evaluate the numerical results in hypothetical dam breach studies (Pilotti et al., 2020). In Álvarez et al. (2017), flow depth hydrographs were compared in the physical model and FLO-2D model at eight locations and calibrated using roughness coefficients. Upon calibration, peak flow depths and timing of the peak flow depths were in good agreement. However, variation in the numerical and physical model results can be seen due to different drawbacks in physical models with regard to the representation of the topography, the difference in scale and surface texture. In Pilotti et al. (2020), the results of two hydrodynamic models, HEC RAS and TELEMAC2D, have been compared for a hypothetical collapse of the Cancano I dam produced as a physical model by De Marchi (1945). The numerical results have shown a good agreement with the physical model and the minor differences are attributed to the inability to reproduce the original bathymetry.

In addition, studies have compared the results of different hydrodynamic models to estimate the accuracy of the results by eliminating the uncertainty associated with the models. In Salt (2019), 2D hydraulic models have been developed from HEC-RAS and DSS-WISE LITE for a Rancho Cielito dam breach with similar terrain files, computational grid and breach parameters. The results have been similar even though HEC RAS and DSS-WISE LITE have different numerical schemes and computational methods.

8 | CONCLUSION

In conclusion, the review shows that high-resolution terrain data and smaller mesh will be required for terrains where local surface variances are significant such as in mountainous regions. In addition, spatially varied mesh sizes and time step can be optimized by iterations of model simulations to achieve sufficient accuracy and computational time. Moreover, the upstream boundary condition, which denotes the dam breach flood inflow to the model is significant in model predictions. Furthermore, the spatially varied roughness coefficients can be selected based on the land cover and land use which is subjected to change in the calibration process. In fact, all the parameters highlighted in this paper can be utilized for analysis in various regions and will govern the accuracy of dam break flood wave propagation.

The datasets that can be used to represent topography show unlimited potential for improvements and the selection of the appropriate dataset and the topographic surface (either DSM or DTM) depends on the terrain characteristics. More research is encouraged on exploring the selection of DSM and DTM for dam break wave modeling. LiDAR data has been an attractive option due to its highest resolution, at the expense of a higher cost. However, global datasets with higher resolution will be a better alternative, especially for flat terrains in the data deficit regions. The use of the new version of ALOS 3D-30 m DEM and TanDEM-X can be explored. The selection of the size, orientation and geometrical characteristics of the grid element affects the accuracy and the speed of the computation and a smaller mesh is recommended in 2D modeling especially near the dam and along the river channel where local surface variations are significant. Furthermore, boundary conditions can be selected based on the study area characteristics and data availability. In fact, normal depth has been the widely used boundary condition in hypothetical dam break analysis. The upstream boundary condition mainly depends on the model set up in which either the dam breach flow hydrograph is used or the dam breach parametric equations specified along with the reservoir water level. Moreover, the model predictions can be efficiently used in risk analysis if the dam breach flow can be estimated on the probabilistic analysis of natural disasters. In addition, the time step is directly connected to model stability and is ideal if it's converged to let flood water cross only one grid cell during the time step. The roughness coefficients have been the main

calibration parameter and the use of spatially varied coefficients is highly recommended. Furthermore, the change of roughness during the propagation of high energetic dam break flow should be investigated for more realistic dam break wave propagation modeling.

Model outputs or the predicted inundation depth, flood velocity, flooding extent and arrival of flood waves at locations where population and infrastructure are at risk in a hypothetical dam breach failure can be utilized to prepare emergency action plans. Moreover, if real time hydraulic models which are calibrated and tested for real time hydraulic inputs, can be operated in major dam control centres, the flood hazard and risk can be identified at a very early stage. In order to optimize such models, the development of global high-resolution datasets which are more affordable for developing countries will be highly beneficial. In addition, the use of 3D models in the simulation of dam break flood flow would be more accurate along with the use of high-resolution data. New research must be focused on minimizing the computational time and need for highly advanced computational resources. Particularly, the application of 3D virtual reality environment to convey the catastrophe of dam disasters is ongoing research to improve citizen engagement in risk aversion.

In summary, the selection of optimum parameters for the model is a main task for a researcher. It must be at the discretion of the researcher, considering the site-specific characteristics, model purpose and budgetary and computational constraints. Furthermore, there has been vast recognition and improvements of the research work in dam break flood inundation modeling due to its obvious usage and applications. On the other hand, the repercussions of dam disasters can be very destructive if such sudden dam disasters are not considered and not prepared to avert the risk. Hence, the hydraulic model predications will be used as a tool to support decision-making for emergency managers. The paper presents the work of the scientific community according to the best of the author's knowledge at the time of writing. New developments and ventures are currently being undertaken; on that account, it is better to be vigilant on the new updates in the software and techniques. Hence, the researchers should always seek new ideas and opportunities that might aid in developing models as realistic as possible while keeping in mind the nonexistence of a perfect model.

AUTHOR CONTRIBUTIONS

P. D. P. O. Peramuna: Conceptualization (lead); formal analysis (lead); investigation (lead); visualization (lead); writing – original draft (lead); writing – review and editing (lead). **N. G. P. B. Neluwala:** Conceptualization (equal); resources (equal); supervision (equal); writing – review and editing (equal). **K. K. Wijesundara:** Conceptualization (equal); resources (equal); supervision (equal); writing – review and editing (equal). **S. DeSilva:** Conceptualization (equal); supervision (equal); writing – review and editing (equal). **Srikanth Venkatesan:** Conceptualization (equal); supervision (equal); writing – review and editing (equal). **P. B. R. Dissanayake:** Conceptualization (equal); resources (equal).

ACKNOWLEDGMENTS

The authors sincerely wish to thank the financial support given by the School of Engineering, RMIT University, Australia and Faculty of Engineering, University of Peradeniya, Sri Lanka along with the provision of the computational resources funded by the Erasmus+ CBHE- CCWater project at the University of Peradeniya, Sri Lanka. Furthermore, reviewers of the Wiley Water journal are highly appreciated for the constructive feedback.

CONFLICT OF INTEREST STATEMENT

The authors have declared no conflicts of interest for this article.

DATA AVAILABILITY STATEMENT

Data sharing is not applicable to this article as no new data were created or analyzed in this study.

ORCID

P. D. P. O. Peramuna  <https://orcid.org/0000-0002-6493-6743>

N. G. P. B. Neluwala  <https://orcid.org/0000-0002-1686-3412>

K. K. Wijesundara  <https://orcid.org/0000-0002-4174-8707>

S. DeSilva  <https://orcid.org/0000-0001-7260-6122>

S. Venkatesan  <https://orcid.org/0000-0001-7382-7576>

P. B. R. Dissanayake  <https://orcid.org/0000-0003-2296-8947>

RELATED WIREs ARTICLE[Flood diversions and bypasses: Benefits and challenges](#)**FURTHER READING**

- Bellos, V., Papageorgaki, I., Kourtis, I., Vangelis, H., Kalogiros, I., & Tsakiris, G. (2020). Reconstruction of a flash flood event using a 2D hydrodynamic model under spatial and temporal variability of storm. *Natural Hazards*, *101*(3), 711–726. <https://doi.org/10.1007/s11069-020-03891-3>
- Dhiman, S., & Patra, K. (2019). Studies of dam disaster in India and equations for breach parameter. *Natural Hazards*, *98*(2), 783–807.
- Sammen, S. S., Mohamed, T. A., Ghazali, A. H., Sidek, L. M., & El-Shafie, A. (2017). An evaluation of existent methods for estimation of embankment dam breach parameters. *Natural Hazards*, *87*(1), 545–566. <https://doi.org/10.1007/s11069-017-2764-z>
- Zhou, X., Chen, Z., Zhou, J., Guo, X., Du, X., & Zhang, Q. (2020). A quantitative risk analysis model for cascade reservoirs overtopping: Principle and application. *Natural Hazards*, *104*(1), 249–277. <https://doi.org/10.1007/s11069-020-04167-6>
- Zhou, Z., Wang, X., Chen, W., Deng, S., & Liu, M. (2017). Numerical simulation of dam-break flooding of cascade reservoirs. *Transactions of Tianjin University*, *23*(6), 570–581. <https://doi.org/10.1007/s12209-017-0073-y>

REFERENCES

- Ahmadian, R., Falconer, R. A., & Wicks, J. (2018). Benchmarking of flood inundation extent using various dynamically linked one- and two-dimensional approaches. *Journal of Flood Risk Management*, *11*, S314–S328. <https://doi.org/10.1111/jfr3.12208>
- Ahmadisharaf, E., Kalyanapu, A. J., Thames, B. A., & Lillywhite, J. (2016). A probabilistic framework for comparison of dam breach parameters and outflow hydrograph generated by different empirical prediction methods. *Environmental Modelling & Software*, *86*, 248–263. <https://doi.org/10.1016/j.envsoft.2016.09.022>
- Albu, L.-M., Enea, A., Iosub, M., & Breabăn, I.-G. (2020). Dam breach size comparison for flood simulations. A HEC-RAS based, GIS approach for Drăcșani Lake, Sitna River, Romania. *Water*, *12*(4), 1090. <https://doi.org/10.3390/w12041090>
- Alcrudo, F., & Mulet, J. (2007). Description of the Tous dam break case study (Spain). *Journal of Hydraulic Research*, *45*(sup1), 45–57. <https://doi.org/10.1080/00221686.2007.9521832>
- Ali, H. T. (2016). *Digital urban terrain characterization for 1D2D hydronamic flood modelling in Kigali, Rwanda* [Master's thesis. University of Twente].
- Álvarez, M., Puertas, J., Peña, E., & Bermúdez, M. (2017). Two-dimensional dam-break flood analysis in data-scarce regions: The case study of Chipembe dam, Mozambique. *Water*, *9*(6), 432. <https://doi.org/10.3390/w9060432>
- Asnaashari, A., Meredith, D., & Scruton, M. (2014). Dam breach inundation analysis using HEC-RAS and GIS—Two case studies in British Columbia, Canada. In *Canadian dam association annual conference, Banff, Alberta*.
- Aureli, F., Maranzoni, A., & Petaccia, G. (2021). Review of historical dam-break events and laboratory tests on real topography for the validation of numerical models. *Water*, *13*(14), 1968. <https://doi.org/10.3390/w13141968>
- Azeez, O., Elfeki, A., Kamis, A. S., & Chaabani, A. (2020). Dam break analysis and flood disaster simulation in arid urban environment: The um Al-Khair dam case study, Jeddah, Saudi Arabia. *Natural Hazards*, *100*, 995–1011. <https://doi.org/10.1007/s11069-019-03836-5>
- Baeza, A., & Mulet, P. (2006). Adaptive mesh refinement techniques for high-order shock capturing schemes for multi-dimensional hydrodynamic simulations. *International Journal for Numerical Methods in Fluids*, *52*(4), 455–471.
- Begnudelli, L., & Sanders, B. F. (2007). Simulation of the St. Francis dam-break flood. *Journal of Engineering Mechanics*, *133*(11), 1200–1212. [https://doi.org/10.1061/\(ASCE\)0733-9399\(2007\)133:11\(1200\)](https://doi.org/10.1061/(ASCE)0733-9399(2007)133:11(1200))
- Belikov, V. V., & Vasil'eva, E. S. (2020). Numerical modeling of a hydrodynamic accident at an earth-and-rockfill dam on the Dyurso River. *Power Technology and Engineering*, *54*(3), 326–331. <https://doi.org/10.1007/s10749-020-01210-1>
- Bellos, C. V., & Sakkas, J. G. (1987). 1-D dam-break flood-wave propagation on dry bed. *Journal of Hydraulic Engineering*, *113*(12), 1510–1524.
- Bellos, V., Tsakiris, V. K., Kopsiaftis, G., & Tsakiris, G. (2020). Propagating dam breach parametric uncertainty in a river reach using the HEC-RAS software. *Hydrology*, *7*(4), 72. <https://doi.org/10.3390/hydrology7040072>
- Bhandari, M. (2017). *One-dimensional (1D) & two-dimensional (2D) dam break analysis and comparison of different breaching parameters using HEC-RAS*. Southern Illinois University at Carbondale.
- Bornschein, A. (2018). Combined influence of terrain Modell and roughness in dam break wave. *E3S Web of Conferences*, *40*, 06026. EDP Sciences.
- Bosa, S., & Petti, M. (2013). A numerical model of the wave that overtopped the Vajont dam in 1963. *Water Resources Management*, *27*, 1763–1779. <https://doi.org/10.1007/s11269-012-0162-6>
- Bricker, J. D., Schwanghart, W., Adhikari, B. R., Moriguchi, S., Roeber, V., & Giri, S. (2017). Performance of models for flash flood warning and Hazard assessment: The 2015 Kali Gandaki landslide dam breach in Nepal. *Mountain Research and Development*, *37*(1), 5–15. <https://doi.org/10.1659/mrd-journal-d-16-00043.1>
- Brunner, G. W. (2020). HEC-RAS River analysis system, 2D modeling User's manual version 6.0.
- Cannata, M., & Marzocchi, R. (2012). Two-dimensional dam break flooding simulation: A GIS-embedded approach. *Natural Hazards*, *61*(3), 1143–1159. <https://doi.org/10.1007/s11069-011-9974-6>

- Cao, Z., Huang, W., Pender, G., & Liu, X. (2014). Even more destructive: cascade dam break floods. *Journal of Flood Risk Management*, 7(4), 357–373. <https://doi.org/10.1111/jfr3.12051>
- Carrivick, J. L. (2010). Dam break–outburst flood propagation and transient hydraulics: A geosciences perspective. *Journal of Hydrology*, 380(3–4), 338–355. <https://doi.org/10.1016/j.jhydrol.2009.11.009>
- Carrivick, J. L., Jones, R., & Keevil, G. (2011). Experimental insights on geomorphological processes within dam break outburst floods. *Journal of Hydrology*, 408(1–2), 153–163. <https://doi.org/10.1016/j.jhydrol.2011.07.037>
- Chow, V., Maidment, D., & Mays, L. W. (1998). *Applied Hydrology*, New York, McGraw-Hill.
- Chow, V. T. (1959). *Open channel hydraulics*. McGraw-Hill.
- Costabile, P., Macchione, F., Natale, L., & Petaccia, G. (2015). Comparison of scenarios with and without bridges and analysis of backwater effect in 1-D and 2-D river flood modeling. *Computer Modeling in Engineering and Sciences*, 109(2), 81–103. <https://doi.org/10.3970/cmcs.2015.109.081>
- Courant, R., Friedrichs, K., & Lewy, H. (1967). On the partial difference equations of mathematical physics. *IBM Journal of Research and Development*, 11(2), 215–234. <https://doi.org/10.1147/rd.112.0215>
- Courty, L. G., Soriano-Monzalvo, J. C., & Pedrozo-Acuña, A. (2019). Evaluation of open-access global digital elevation models (AW3D30, SRTM, and ASTER) for flood modelling purposes. *Journal of Flood Risk Management*, 12(S1), e12550. <https://doi.org/10.1111/jfr3.12550>
- Dasallas, L., Kim, Y., & An, H. (2019). Case study of HEC-RAS 1D–2D coupling simulation: 2002 Baeksan flood event in Korea. *Water*, 11(10), 2048. <https://doi.org/10.3390/w11102048>
- De Marchi, G. (1945). Sull'onda di piena che seguirebbe al crollo della diga di Cancano. [On the dam-break wave resulting from the collapse of the Cancano dam]. *L'Energia Elettrica*, 22(1), 319–340.
- Evans, A. D., Gardner, K. H., Greenwood, S., & Still, B. (2022). UAV and structure-from-motion photogrammetry enhance River restoration monitoring: A dam removal study. *Drones*, 6(5), 100. <https://doi.org/10.3390/drones6050100>
- Farooq, M., Shafique, M., & Khattak, M. S. (2019). Flood hazard assessment and mapping of river swat using HEC-RAS 2D model and high-resolution 12-m TanDEM-X DEM (WorldDEM). *Natural Hazards*, 97(2), 477–492. <https://doi.org/10.1007/s11069-019-03638-9>
- Farr, T. G., Rosen, P. A., Caro, E., Crippen, R., Duren, R., Hensley, S., Kobrick, M., Paller, M., Rodriguez, E., Roth, L., Seal, D., Shaffer, S., Shimada, J., Umland, J., Werner, M., Oskin, M., Burbank, D., & Alsdorf, D. (2007). The shuttle radar topography mission. *Reviews of Geophysics*, 45(2), RG2004. <https://doi.org/10.1029/2005rg000183>
- Froehlich, D. C. (2008). Embankment dam breach parameters and their uncertainties. *Journal of Hydraulic Engineering*, 134(12), 1708–1721. [https://doi.org/10.1061/\(ASCE\)0733-9429\(2008\)134:12\(1708\)](https://doi.org/10.1061/(ASCE)0733-9429(2008)134:12(1708))
- Gaagai, A., Aouissi, H. A., Krauklis, A. E., Burlakovs, J., Athamena, A., Zekker, I., Boudoukha, A., Benaabidate, L., & Chenchouni, H. (2022). Modeling and risk analysis of dam-break flooding in a semi-arid montane watershed: A case study of the Yabous dam, Northeastern Algeria. *Water*, 14(5), 767. <https://doi.org/10.3390/w14050767>
- Gallegos, H. A., Schubert, J. E., & Sanders, B. F. (2009). Two-dimensional, high-resolution modeling of urban dam-break flooding: A case study of Baldwin Hills, California. *Advances in Water Resources*, 32(8), 1323–1335. <https://doi.org/10.1016/j.advwatres.2009.05.008>
- Garcia, M., & Popiolek, T. (2014). Adaptive mesh refinement in the dam-break problems. *10th World Congress on Computational Mechanics, Blucher Mechanical Engineering Proceedings, 1*, 4163–4175. <https://doi.org/10.1016/meceng-wccm2012-19753>
- Garcia-Navarro, P., Fras, A., & Villanueva, I. (1999). Dam-break flow simulation: Some results for one-dimensional models of real cases. *Journal of Hydrology*, 216(3–4), 227–247. [https://doi.org/10.1016/S0022-1694\(99\)00007-4](https://doi.org/10.1016/S0022-1694(99)00007-4)
- Gottardi, G., & Venutelli, M. (2004). Central scheme for two-dimensional dam-break flow simulation. *Advances in Water Resources*, 27(3), 259–268. <https://doi.org/10.1016/j.advwatres.2003.12.006>
- Grohmann, C. H. (2018). Evaluation of TanDEM-X DEMs on selected Brazilian sites: Comparison with SRTM, ASTER GDEM and ALOS AW3D30. *Remote Sensing of Environment*, 212, 121–133. <https://doi.org/10.1016/j.rse.2018.04.043>
- Grover, P., Naumov, A., & Khayer, Y. (2013). Comparison of 1D and 2D models for dam break flow: Simulations for two different river systems. In XXth TELEMAC-MASCARET. User Conference.
- Haltas, I., Elçi, S., & Tayfur, G. (2016). Numerical simulation of flood wave propagation in two-dimensions in densely populated urban areas due to dam break. *Water Resources Management*, 30(15), 5699–5721. <https://doi.org/10.1007/s11269-016-1344-4>
- Haltas, I., Tayfur, G., & Elçi, S. (2016). Two-dimensional numerical modeling of flood wave propagation in an urban area due to Ürkmez dam-break, İzmir, Turkey. *Natural Hazards*, 81(3), 2103–2119. <https://doi.org/10.1007/s11069-016-2175-6>
- Hervouet, J. M., & Petitjean, A. (1999). Malpasset dam-break revisited with two-dimensional computations. *Journal of Hydraulic Research*, 37(6), 777–788. <https://doi.org/10.1080/00221689909498511>
- Jančíková, A., & Unucka, J. (2015). DTM impact on the results of dam break simulation in 1D hydraulic models. In K. Růžicková & T. Inspektor (Eds.), *Surface Models for Geosciences. Lecture Notes in Geoinformation and Cartography* (pp. 125–136). Springer, Cham. 125–136. https://doi.org/10.1007/978-3-319-18407-4_11
- Jonkman, S. N., & Vrijling, J. K. (2008). Loss of life due to floods. *Journal of Flood Risk Management*, 1(1), 43–56. <https://doi.org/10.1111/j.1753-318X.2008.00006.x>
- Kidyaveva, V., Chernomorets, S., Krylenko, I., Wei, F., Petrakov, D., Su, P., Yang, H., & Xiong, J. (2017). Modeling potential scenarios of the Tangjiashan lake outburst and risk assessment in the downstream valley. *Frontiers of Earth Science*, 11(3), 579–591. <https://doi.org/10.1007/s11707-017-0640-5>
- Kim, B., & Sanders, B. F. (2016). Dam-break flood model uncertainty assessment: Case study of extreme flooding with multiple dam failures in Gangneung, South Korea. *Journal of Hydraulic Engineering*, 142(5), 05016002. [https://doi.org/10.1061/\(asce\)hy.1943-7900.0001097](https://doi.org/10.1061/(asce)hy.1943-7900.0001097)

- Kim, B., Sanders, B. F., Schubert, J. E., & Famiglietti, J. S. (2014). Mesh type tradeoffs in 2D hydrodynamic modeling of flooding with a Godunov-based flow solver. *Advances in Water Resources*, 68, 42–61. <https://doi.org/10.1016/j.advwatres.2014.02.013>
- Krieger, G., Moreira, A., Fiedler, H., Hajnsek, I., Werner, M., Younis, M., & Zink, M. (2007). TanDEM-X: A satellite formation for high-resolution SAR interferometry. *IEEE Transactions on Geoscience and Remote Sensing*, 45(11), 3317–3341. <https://doi.org/10.1109/tgrs.2007.900693>
- Lakhlifi, Y., Daoudi, S., & Boushaba, F. (2018). Dam-break computations by a dynamical adaptive finite volume method. *Journal of Applied Fluid Mechanics*, 11(6), 1543–1556.
- Latrubesse, E. M., Park, E., Sieh, K., Dang, T., Lin, Y. N., & Yun, S.-H. (2020). Dam failure and a catastrophic flood in the Mekong basin (Bolaven plateau), southern Laos, 2018. *Geomorphology*, 362, 107221. <https://doi.org/10.1016/j.geomorph.2020.107221>
- Lavoie, B., & Mahdi, T.-F. (2017). Comparison of two-dimensional flood propagation models: SRH-2D and Hydro_AS-2D. *Natural Hazards*, 86, 1207–1222. <https://doi.org/10.1007/s11069-016-2737-7>
- Li, J., Cao, Z., Pender, G., & Liu, Q. (2013). A double layer-averaged model for dam-break flows over mobile bed. *Journal of Hydraulic Research*, 51(5), 518–534. <https://doi.org/10.1080/00221686.2013.812047>
- Li, W., Zhu, J., Fu, L., Zhu, Q., Guo, Y., & Gong, Y. (2021). A rapid 3D reproduction system of dam-break floods constrained by post-disaster information. *Environmental Modelling & Software*, 139, 104994. <https://doi.org/10.1016/j.envsoft.2021.104994>
- Luo, J., Xu, W., Tian, Z., & Chen, H. (2019). Numerical simulation of cascaded dam-break flow in downstream reservoir. *Proceedings of the Institution of Civil Engineers—Water Management*, 172(2), 55–67. <https://doi.org/10.1680/jwama.15.00088>
- Macchione, F., Costabile, P., Costanzo, C., de Lorenzo, G., & Razdar, B. (2016). Dam breach modelling: Influence on downstream water levels and a proposal of a physically based module for flood propagation software. *Journal of Hydroinformatics*, 18(4), 615–633. <https://doi.org/10.2166/hydro.2015.250>
- Macchione, F., & Viggiani, G. (2004). Simple modelling of dam failure in a natural river. *Proceedings of the Institution of Civil Engineers - Water Management*, 157(1), 53–60. Thomas Telford Ltd. <https://doi.org/10.1680/wama.2004.157.1.53>
- Mandlbürger, G., Hauer, C., Höfle, B., Habersack, H., & Pfeifer, N. (2009). Optimisation of LiDAR derived terrain models for river flow modelling. *Hydrology and Earth System Sciences*, 13(8), 1453–1466. <https://doi.org/10.5194/hess-13-1453-2009>
- Marangoz, H. O., & Anilan, T. (2022). Two-dimensional modeling of flood wave propagation in residential areas after a dam break with application of diffusive and dynamic wave approaches. *Natural Hazards*, 110(1), 429–449. <https://doi.org/10.1007/s11069-021-04953-w>
- McClellan, F., Dawson, R., & Kilsby, C. (2020). Implications of using global digital elevation models for flood risk analysis in cities. *Water Resources Research*, 56(10), e2020WR028241. <https://doi.org/10.1029/2020WR028241>
- Meesuk, V., Vojinovic, Z., Mynett, A. E., & Abdullah, A. F. (2015). Urban flood modelling combining top-view LiDAR data with ground-view SfM observations. *Advances in Water Resources*, 75, 105–117. <https://doi.org/10.1016/j.advwatres.2014.11.008>
- Mhmood, H. H., Yilmaz, M., & Sulaiman, S. O. (2022). Simulation of the flood wave caused by hypothetical failure of the Haditha dam. *Journal of Applied Water Engineering and Research*, 11(1), 66–76. <https://doi.org/10.1080/23249676.2022.2050312>
- Nkwunonwo, U., Whitworth, M., & Baily, B. (2020). A review of the current status of flood modelling for urban flood risk management in the developing countries. *Scientific African*, 7, e00269. <https://doi.org/10.1016/j.sciaf.2020.e00269>
- O'Loughlin, F. E., Paiva, R. C., Durand, M., Alsdorf, D., & Bates, P. (2016). A multi-sensor approach towards a global vegetation corrected SRTM DEM product. *Remote Sensing of Environment*, 182, 49–59. <https://doi.org/10.1016/j.rse.2016.04.018>
- Ongdas, N., Akiyanova, F., Karakulov, Y., Muratbayeva, A., & Zinabdin, N. (2020). Application of HEC-RAS (2D) for flood Hazard maps generation for Yesil (Ishim) river in Kazakhstan. *Water*, 12(10), 2672. <https://doi.org/10.3390/w12102672>
- Ozmen-Cagatay, H., Turhan, E., & Kocaman, S. (2022). An experimental investigation of dam-break induced flood waves for different density fluids. *Ocean Engineering*, 243, 110227. <https://doi.org/10.1016/j.oceaneng.2021.110227>
- Palu, M. C., & Julien, P. Y. (2020). Test and improvement of 1D routing algorithms for dam-break floods. *Journal of Hydraulic Engineering*, 146(6), 04020043. [https://doi.org/10.1061/\(ASCE\)HY.1943-7900.0001755](https://doi.org/10.1061/(ASCE)HY.1943-7900.0001755)
- Pappenberger, F., Beven, K., Horritt, M., & Blazkova, S. (2005). Uncertainty in the calibration of effective roughness parameters in HEC-RAS using inundation and downstream level observations. *Journal of Hydrology*, 302(1–4), 46–69. <https://doi.org/10.1016/j.jhydrol.2004.06.036>
- Patel, D. P., Ramirez, J. A., Srivastava, P. K., Bray, M., & Han, D. (2017). Assessment of flood inundation mapping of Surat city by coupled 1D/2D hydrodynamic modeling: A case application of the new HEC-RAS 5. *Natural Hazards*, 89(1), 93–130. <https://doi.org/10.1007/s11069-017-2956-6>
- Pilotti, M., Maranzoni, A., Milanese, L., Tomirotti, M., & Valerio, G. (2014). Dam-break modeling in alpine valleys. *Journal of Mountain Science*, 11(6), 1429–1441. <https://doi.org/10.1007/s11629-014-3042-0>
- Pilotti, M., Maranzoni, A., Tomirotti, M., & Valerio, G. (2011). 1923 Gleno dam break: Case study and numerical modeling. *Journal of Hydraulic Engineering*, 137(4), 480–492. [https://doi.org/10.1061/\(asce\)hy.1943-7900.0000327](https://doi.org/10.1061/(asce)hy.1943-7900.0000327)
- Pilotti, M., Milanese, L., Bacchi, V., Tomirotti, M., & Maranzoni, A. (2020). Dam-break wave propagation in Alpine Valley with HEC-RAS 2D: Experimental Cancano test case. *Journal of Hydraulic Engineering*, 146(6), 05020003. [https://doi.org/10.1061/\(asce\)hy.1943-7900.0001779](https://doi.org/10.1061/(asce)hy.1943-7900.0001779)
- Psomiadis, E., Tomanis, L., Kavvadias, A., Soulis, K. X., Charizopoulos, N., & Michas, S. (2021). Potential dam breach analysis and flood wave risk assessment using HEC-RAS and remote sensing data: A multicriteria approach. *Water*, 13(3), 364. <https://doi.org/10.3390/w13030364>
- Quecedo, M., Pastor, M., Herreros, M. I., Merodo, J. A. F., & Zhang, Q. (2005). Comparison of two mathematical models for solving the dam break problem using the FEM method. *Computer Methods in Applied Mechanics and Engineering*, 194(36–38), 3984–4005. <https://doi.org/10.1016/j.cma.2004.09.011>

- Rabus, B., Eineder, M., Roth, A., & Bamler, R. (2003). The shuttle radar topography mission—A new class of digital elevation models acquired by spaceborne radar. *ISPRS Journal of Photogrammetry and Remote Sensing*, 57(4), 241–262. [https://doi.org/10.1016/s0924-2716\(02\)00124-7](https://doi.org/10.1016/s0924-2716(02)00124-7)
- Říha, J., Kotaška, S., & Petruľa, L. (2020). Dam break modeling in a cascade of small earthen dams: Case study of the Čizina river in The Czech Republic. *Water*, 12(8), 2309. <https://doi.org/10.3390/w12082309>
- Robb, D., & Vasquez, J. (2015). Numerical simulation of dam-break flows using depth-averaged hydrodynamic and three-dimensional CFD models. *Proceeding of Canadian Society for Civil Engineering 22nd Hydrotechnical Conference*, 27–36.
- Salt, D. V. (2019). *A comparison of HEC-RAS and DSS-WISE Lite 2D hydraulic models for a rancho Cielito dam breach*. [Master's thesis. California State University].
- Sarchani, S., & Koutroulis, A. G. (2022). Probabilistic dam breach flood modeling: The case of valsamiotis dam in crete. *Natural Hazards*, 114(2), 1763–1814. <https://doi.org/10.1007/s11069-022-05446-0>
- Sattar, A., Goswami, A., & Kulkarni, A. V. (2019). Hydrodynamic moraine-breach modeling and outburst flood routing—A hazard assessment of the south Lhonak lake, Sikkim. *Sci Total Environ*, 668, 362–378. <https://doi.org/10.1016/j.scitotenv.2019.02.388>
- Scapozza, C., Ambrosi, C., Cannata, M., & Strozzi, T. (2019). Glacial lake outburst flood hazard assessment by satellite earth observation in the Himalayas (Chomolhari area, Bhutan). *Geographica Helvetica*, 74(1), 125–139. <https://doi.org/10.5194/gh-74-125-2019>
- Schubert, J. E., Sanders, B. F., Smith, M. J., & Wright, N. G. (2008). Unstructured mesh generation and landcover-based resistance for hydrodynamic modeling of urban flooding. *Advances in Water Resources*, 31(12), 1603–1621. <https://doi.org/10.1016/j.advwatres.2008.07.012>
- Shigematsu, T., Liu, P. L.-F., & Oda, K. (2004). Numerical modeling of the initial stages of dam-break waves. *Journal of Hydraulic Research*, 42(2), 183–195. <https://doi.org/10.1080/00221686.2004.9728381>
- Shustikova, I., Domeneghetti, A., Neal, J. C., Bates, P., & Castellarin, A. (2019). Comparing 2D capabilities of HEC-RAS and LISFLOOD-FP on complex topography. *Hydrological Sciences Journal*, 64(14), 1769–1782. <https://doi.org/10.1080/02626667.2019.1671982>
- Shustikova, I., Neal, J. C., Domeneghetti, A., Bates, P. D., Vorogushyn, S., & Castellarin, A. (2020). Levee breaching: A new extension to the LISFLOOD-FP model. *Water*, 12(4), 942. <https://doi.org/10.3390/w12040942>
- Soares-Frazão, S., Canelas, R., Cao, Z., Cea, L., Chaudhry, H. M., Die Moran, A., El Kadi, K., Ferreira, R., Cadórniga, I. F., Gonzalez-Ramirez, N., Greco, M., Huang, W., Imran, J., Le Coz, J., Marsooli, R., Paquier, A., Pender, G., Pontillo, M., Puertas, J., ... Zech, Y. (2012). Dam-break flows over mobile beds: Experiments and benchmark tests for numerical models. *Journal of Hydraulic Research*, 50(4), 364–375. <https://doi.org/10.1080/00221686.2012.689682>
- Spero, H. R., Vazquez-Lopez, I., Miller, K., Joshaghani, R., Cutchin, S., & Enterkine, J. (2022). Drones, virtual reality, and modeling: Communicating catastrophic dam failure. *International Journal of Digital Earth*, 15(1), 585–605. <https://doi.org/10.1080/17538947.2022.2041116>
- Swartenbroekx, C., Zech, Y., & Soares-Frazão, S. (2013). Two-dimensional two-layer shallow water model for dam break flows with significant bed load transport. *International Journal for Numerical Methods in Fluids*, 73(5), 477–508. <https://doi.org/10.1002/flid.3809>
- Tadono, T., Ishida, H., Oda, F., Naito, S., Minakawa, K., & Iwamoto, H. (2014). Precise global DEM generation by ALOS PRISM. *ISPRS Annals of the Photogrammetry, Remote Sensing and Spatial Information Sciences*, 2(4), 71–76. <https://doi.org/10.5194/isprsannals-II-4-71-2014>
- Tedla, M. G., Cho, Y., & Jun, K. (2021). Flood mapping from dam break due to peak inflow: A coupled rainfall–runoff and hydraulic models approach. *Hydrology*, 8(2), 89. <https://doi.org/10.3390/hydrology8020089>
- Urzică, A., Miħu-Pintilie, A., Stoleriu, C. C., Cimpianu, C. I., Huřanu, E., Pricop, C. I., & Grozavu, A. (2021). Using 2D HEC-RAS modeling and embankment dam break scenario for assessing the flood control capacity of a multi-reservoir system (NE Romania). *Water*, 13(1), 57. <https://doi.org/10.3390/w13010057>
- United States Army Corps of Engineers (1981). *Interim guidelines for estimating n values on flood plains*.
- Vacondio, R., Aureli, F., Ferrari, A., Mignosa, P., & Palu, A. D. (2016). Simulation of the January 2014 flood on the Secchia River using a fast and high-resolution 2D parallel shallow-water numerical scheme. *Natural Hazards*, 80, 103–125. <https://doi.org/10.1007/s11069-015-1959-4>
- Valiani, A., Caleffi, V., & Zanni, A. (2002). Case study: Malpasset dam-break simulation using a two-dimensional finite volume method. *Journal of Hydraulic Engineering*, 128(5), 460–472. [https://doi.org/10.1061/\(ASCE\)1084-0699\(2002\)128:5\(460\)](https://doi.org/10.1061/(ASCE)1084-0699(2002)128:5(460))
- Wang, B., Chen, Y., Wu, C., Dong, J., Ma, X., & Song, J. (2016). A semi-analytical approach for predicting peak discharge of floods caused by embankment dam failures. *Hydrological Processes*, 30(20), 3682–3691. <https://doi.org/10.1002/hyp.10896>
- Wang, K., Yang, P., Yu, G., Yang, C., & Zhu, L. (2020). 3D numerical modelling of tailings dam breach run out flow over complex terrain: A multidisciplinary procedure. *Water*, 12(9), 2538. <https://doi.org/10.3390/w12092538>
- Xanthopoulos, T., & Koutitas, C. (2010). Numerical simulation of a two dimensional flood wave propagation due to dam failure. *Journal of Hydraulic Research*, 14(4), 321–331. <https://doi.org/10.1080/00221687609499664>
- Yamazaki, D., Ikeshima, D., Sosa, J., Bates, P. D., Allen, G. H., & Pavelsky, T. M. (2019). MERIT hydro: A high-resolution global hydrography map based on latest topography dataset. *Water Resources Research*, 55(6), 5053–5073. <https://doi.org/10.1029/2019WR024873>
- Yamazaki, D., Ikeshima, D., Tawatari, R., Yamaguchi, T., O'Loughlin, F., Neal, J. C., Sampson, C. C., Kanae, S., & Bates, P. D. (2017). A high-accuracy map of global terrain elevations. *Geophysical Research Letters*, 44(11), 5844–5853. <https://doi.org/10.1002/2017gl072874>
- Yang, F. L., Zhang, X. F., & Tan, G. M. (2007). One-and two-dimensional coupled hydrodynamics model for dam break flow. *Journal of Hydrodynamics*, 19(6), 769–775. [https://doi.org/10.1016/S1001-6058\(08\)60016-5](https://doi.org/10.1016/S1001-6058(08)60016-5)
- Yochum, S. E., Goertz, L. A., & Jones, P. H. (2008). Case study of the big bay dam failure: Accuracy and comparison of breach predictions. *Journal of Hydraulic Engineering*, 134(9), 1285–1293. [https://doi.org/10.1061/\(ASCE\)0733-9429\(2008\)134:9\(1285\)](https://doi.org/10.1061/(ASCE)0733-9429(2008)134:9(1285))

- Yudianto, D., Ginting, B. M., Sanjaya, S., Rusli, S. R., & Wicaksono, A. (2021). A framework of dam-break Hazard risk mapping for a data-sparse region in Indonesia. *ISPRS International Journal of Geo-Information*, *10*(3), 110. <https://doi.org/10.3390/ijgi10030110>
- Zhang, T., Peng, L., & Feng, P. (2018). Evaluation of a 3D unstructured-mesh finite element model for dam-break floods. *Computers & Fluids*, *160*, 64–77. <https://doi.org/10.1016/j.compfluid.2017.10.013>
- Zhong, Q., Wu, W., Chen, S., & Wang, M. (2016). Comparison of simplified physically based dam breach models. *Natural Hazards*, *84*(2), 1385–1418. <https://doi.org/10.1007/s11069-016-2492-9>
- Zhong, Q. M., Chen, S. S., Deng, Z., & Mei, S. A. (2019). Prediction of overtopping-induced breach process of cohesive dams. *Journal of Geotechnical and Geoenvironmental Engineering*, *145*(5), 04019012. [https://doi.org/10.1061/\(asce\)gt.1943-5606.0002035](https://doi.org/10.1061/(asce)gt.1943-5606.0002035)

How to cite this article: Peramuna, P. D. P. O., Neluwala, N. G. P. B., Wijesundara, K. K., DeSilva, S., Venkatesan, S., & Dissanayake, P. B. R. (2024). Review on model development techniques for dam break flood wave propagation. *WIREs Water*, *11*(2), e1688. <https://doi.org/10.1002/wat2.1688>